

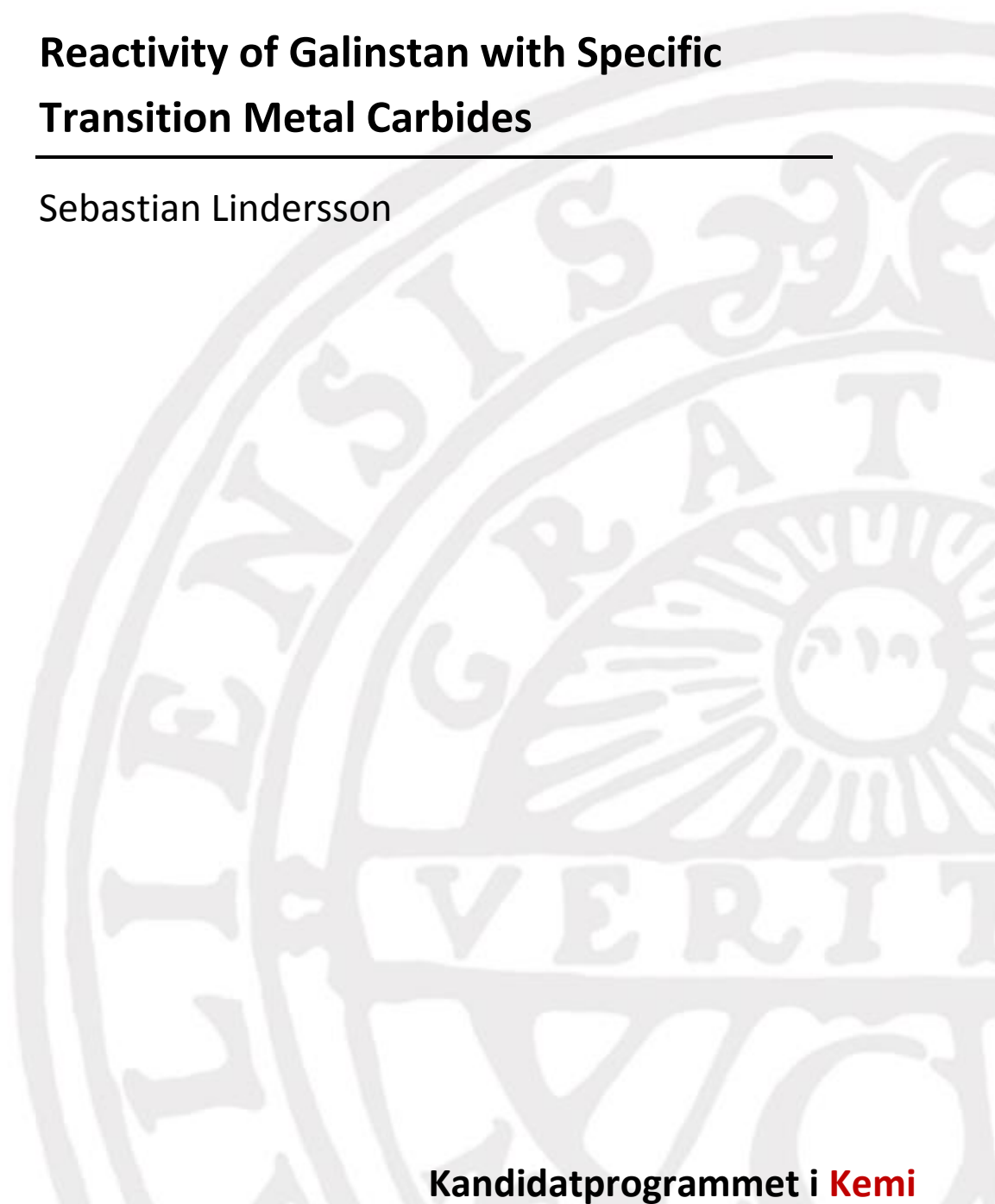


UPPSALA
UNIVERSITET

Examensarbete 15 hp
Mars 2014

Reactivity of Galinstan with Specific Transition Metal Carbides

Sebastian Lindersson



Kandidatprogrammet i **Kemi**

Bachelor Programme in Chemistry

Abstract

Reactivity of Galinstan with Specific Transition Metal Carbides

Sebastian Lindersson

This project examines the reactivity of “Galinstan” against specific transition metal carbide (MeC_x) films deposited on aluminum (Al) thin films. Galinstan is a non-toxic liquid metal alloy at room temperature, consisting of gallium, indium and tin, and has been studied in order to replace mercury in its’ applications, as well as new applications as microfluidics. However, Galinstan reacts with other conductive materials such as Al, therefore it is interesting to find solutions to prevent this. Thus, MeC_x films were tested as barriers between Galinstan and Al. Two approaches of analysis have been performed: X-Ray Diffraction (XRD) was employed to identify potential phase changes of the MeC_x films upon Galinstan exposure, and X-ray Photoelectron Spectroscopy (XPS) for determining whether the MeC_x films were penetrated by Galinstan or not. It was seen that the MeC_x films protected Al from reacting with Galinstan. However, the MeC_x films proved to be sensitive to mechanical damages, and so were the Al films. By scratching a MeC_x surface with a pipette tip, Galinstan would react with the Al underneath, resulting in crack formation. XPS analysis showed that there were no chemical changes upon scratching the MeC_x surface, and the oxide layer remained intact. This lead to the conclusion that mechanical damages was the cause of the reactions between Galinstan and Al. It is believed that scratching the MeC_x surface would allow Galinstan to diffuse through and react with the Al underneath. Hence, further studies on what happens when the surface gets scratched is needed. For this matter, Scanning Electron Microscopy (SEM) can be applied. It was also shown that the presence of water would enhance the reaction between Galinstan and Al. This could be prevented if water could not condense to the samples. The $\text{Cr-C}_{\text{poor}}$ film showed the best resistance towards Galinstan exposure, and Galinstan barely adhered to this film. Zr-C and $\text{Cr-C}_{\text{rich}}$ protected Al as well, while Ti-C and Nb-C did not.

Supervisor: Erik Lewin

Topic reviewer: Martin Häggblad Sahlberg

Examiner: Helena Grennberg

Table of Contents

1. Introduction	4
1.1. Motivation and Objective	4
1.2. Galinstan	4
1.3. Aluminum	5
1.4. Transition metal carbides	6
2. Experimental details	7
2.1. Equipments	7
2.2. Materials	9
2.3. Initial experiments	10
2.3.1. Al films	10
2.3.2. CrC films	11
2.4. Main experiments	11
3. Results	11
3.1. Initial experiments	12
3.1.1 Al films	12
3.1.2. Cr-C films	12
3.2. Al films	14
3.3. Cr-C films	15
3.3.1. Cr-C _{rich} films	15
3.3.2. Cr-C _{poor} films	18
3.4. Ti-C films	20
3.5. Nb-C films	22
3.6. Zr-C films	23
3.7. Scratching with pipette	26
4. Discussion and summary	27
5. Conclusions	29
6. Acknowledgements	31
7. References	32

1. Introduction

1.1. Motivation and Objective

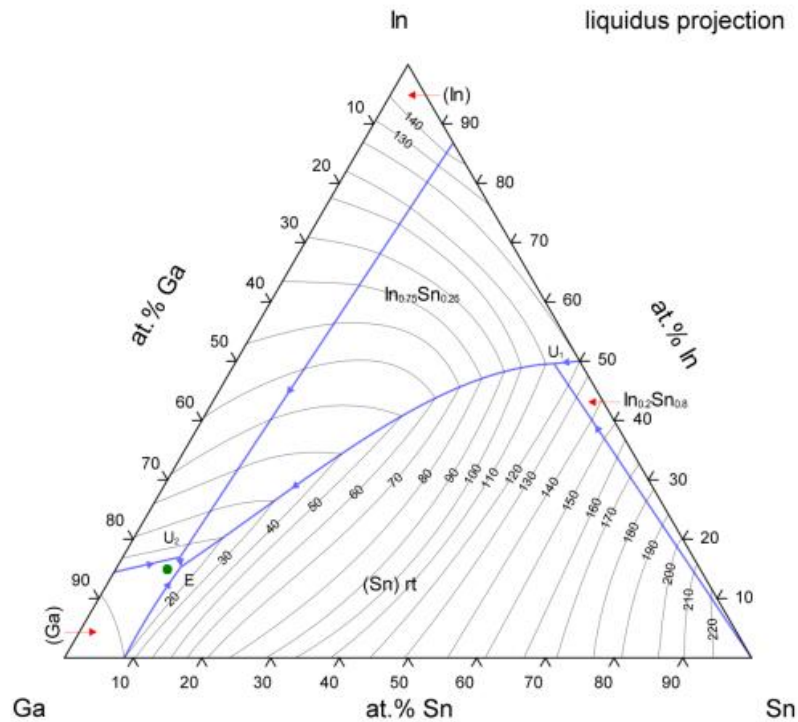
Electronics are highly demanded products in today's society that have been developed remarkably throughout the years. A very interesting field of electronics is microfluidic electronics – liquids with good electrical and thermal conductivity that are employed in electronic devices on the micrometer scale [1]. Some great advantages that microfluidics possesses compared to solid conductive materials (e.g. copper, aluminum, etc.) is mechanical deformability as well as low energy consumption. What makes microfluidic electronics very attractive for research and development [1]. Microfluidic electronics was first discovered by H. Hollerith in 1894 [1,2].

The liquid metal alloy “Galinstan” (Ga-In-Sn alloy, see section 1.2. *Galinstan*) is commercially made by Geratherm Medical GA, Germany. It has been used as a replacement of mercury in thermometers [3], and research is currently employed in order to adapt this liquid metal alloy in microfluidic electronics. For instance, a study by Hu *et al.* have shown that Galinstan works excellently as electrical interconnection in flexible sensor-skin (microfluidic channels) [4]. A large concern however, is that Galinstan reacts with other conductive metals, such as aluminum (Al). Galinstan is corrosive against metals [5], which will lead to degeneration of other metal conductors in electronics by using Galinstan as a microfluidic conductor.

The objective with this project has been to test the reactivity of Galinstan with specific transition metal carbide thin films in comparison to Al. This was done with simple laboratory set-ups in both ambient conditions as well as at elevated temperatures (150 °C). A camera was employed in order to follow reactions over time.

1.2. Galinstan

Galinstan is a ternary eutectic alloy that is liquid down to -19 °C and is commercially made by Geratherm Medical GA, Germany [5]. It contains 78 atomic percents (at%) of gallium (Ga), 15 at% of indium (In) and 7 at% of tin (Sn) [6,7], though a few further components exist that are not labeled. This can be seen by interpreting the phase diagram of the Ga-In-Sn ternary alloy (which has no eutectic at such compositions), see figure 1 [8]. What makes Galinstan interesting is firstly that it is a nontoxic liquid metal alloy at room temperature, and secondly, it shows good electrical as well as thermal conductivity [5]. These features is what makes Galinstan a possible replacement for mercury, an otherwise very toxic and environmentally harmful element. One commercial application where Galinstan has replaced Mercury is thermometers [3]. Galinstan has also been studied for other applications, such as in microdevices [7] and heat sinks/coolants [9].



© ASM International 2006. Diagram No. 990059

Figure 1 Ternary phase diagram of the Ga-In-Sn system. The eutectic E (bottom left corner) is not the same as for Galinstan [8]. Galinstan's eutectic point, according to the given chemical compositions of Ga, In and Sn, is marked with a green point (next to the E).

There are a few problems that prevent beneficial application of Galinstan in most systems. Galinstan is conceived as a very "sticky" liquid that adheres to almost everything [6]. However this is not a property of Galinstan by itself, in fact, gallium within the liquid oxidizes immediately after exposure to ambient air [7]. This gallium oxide (mainly the more stable Ga_2O_3 , but Ga_2O also exists) starts to form on top of the surface of Galinstan (e.g. the surface of a Galinstan drop) [10]. This causes the surface to become more gel-like and therefore sticky [6]. This may cause problems when it comes to applying Galinstan in e.g. microdevices, where it must function as a non-adhering liquid [7].

1.3. Aluminum

Aluminum (Al) is a metallic element which has a low density and a good resistance to atmospheric corrosion. This is due to that Al forms a protective oxide film (Al_2O_3) which stops the metal from oxidizing further [11]. These features make Al interesting in terms of building and construction, as well as for packaging and transport [11]. What is the most interesting is that Al is a good electrical conductive material which is also cheap (in comparison to Copper and Gold) which is beneficial for electronics [11,12].

1.4. Transition metal carbides

Transition metal carbides (MeC_x , where index x indicates a varied stoichiometry of carbon) consist of a transition metal (Me) and carbon (C), and many of them was first synthesized by H. Moissan in 1893 [13,14]. These materials are known to have great hardness as well as very good electrical and thermal conductivity [13]. They are also generally inert against non-oxidizing acids [13] and highly stable compounds [15], which has led to the interest of testing MeC_x films as barriers between Galinstan and Al. Depending on the choice of deposition conditions (such as compositions of Me and C), different microstructures could be obtained: Single phase crystalline carbides (MeC_x), nanocomposites of nanocrystalline carbide and amorphous carbon (nc- $\text{MeC}_x/\text{a-C}$) or amorphous coatings [16]. Nanocomposite carbides consist of either two nanocrystalline (nc-) phases or nc-carbide grains surrounded by an amorphous matrix, such as amorphous carbon (a-C) [17, 18]. An amorphous solid is a solid material which has no crystalline structure. However, amorphous solids have a short-range order, unlike crystalline solids that have both a short- and long-range order [19], see figure 2. Because of this, amorphous solids will have no imperfections (e.g. grains) which would otherwise arise for crystalline solids due to their long-range orders [20]. Amorphous solids will therefore have smoother surfaces due to the lack of imperfections (i.e. no surface defects).

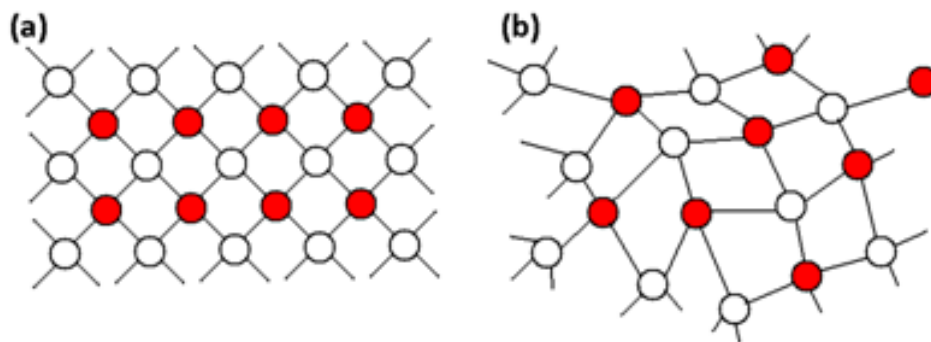


Figure 2 Sketch of (a) a crystalline solid with a short- and long-range order of atoms, and (b) an amorphous solid with short-range order of atoms.

2. Experimental details

2.1. Equipments

Galinstan from Geratherm Medical AG (732 g; 2013-01-23) was used for all experiments.

Experiments were performed by using a petri dish, in which the samples were placed. In order to apply Galinstan on the films, an automatic pipette (Biohit Proline, 5-50 μ l) was used together with plastic pipette tips. A volume of 25 μ l was used for all experiments, which seemed to be reasonable in terms of Galinstan consumption.

The camera with the interval timer was programmed both at the start and during the experiments – Photographs were taken more frequently when reaction occurred. The following programs were used:

- Program 1: 1 photo/min for 1 hour, starting right after application of Galinstan drop.
- Program 2: 1 photo/h for 23 hours, starting right after Program 1.

These programs were evaluated from observations of test experiments with CrC. The total time of photographing was decided to be 24 hours due to battery capacity restrictions. For the experiments at elevated temperatures (described in section 2.4. *Main experiments*), a different photo program was used:

- Program 3: 1 photo/10min for 1 hour, followed by 1 photo/h for 6 hours.

Films (the whole film) were analyzed with Grazing Incidence X-Ray Diffraction (GIXRD) using a Siemens D5000 diffractometer. For all measurements, an incidence angle of 1° was used, together with an increment of 0.1° and a step time of 2.0 s/step. XRD was employed for phase identification of unexposed samples and samples exposed to Galinstan. It was thus used in order to determine whether the phases of the films would change by the presence of Galinstan.

An example of a diffractogram of an Al film (blank sample) can be seen in figure 3. By comparing with specific references, it was possible to determine which crystal structure the element (i.e. Al) had. As expected, the Al film had a cubic structure [21].

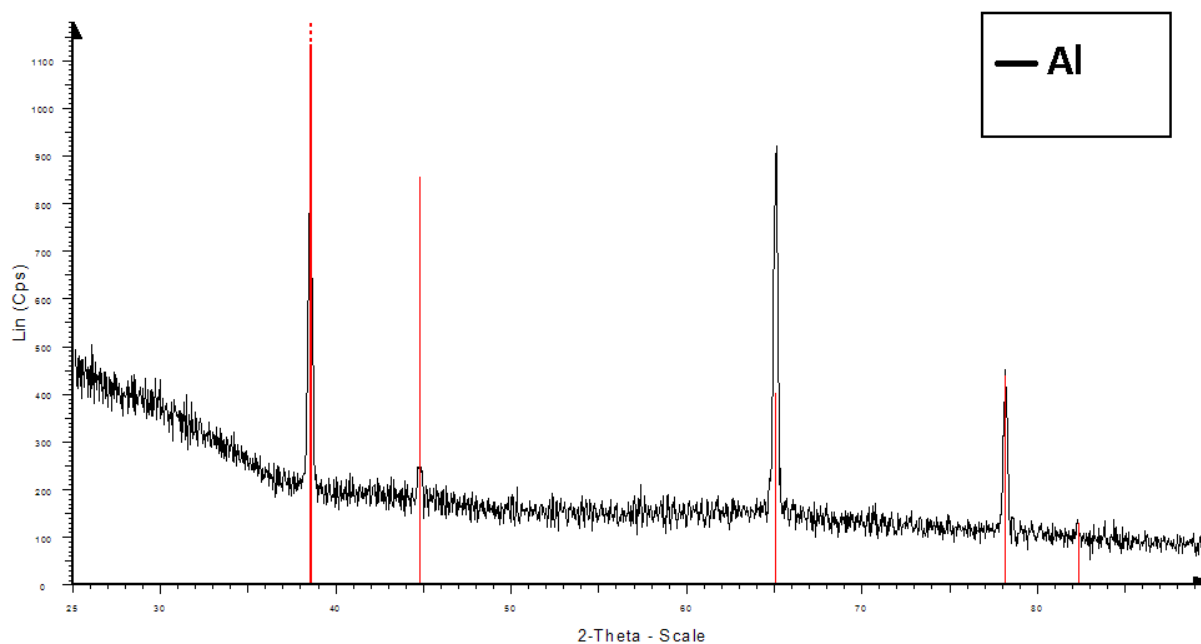


Figure 3 Diffractogram of an Al film (blank) with reference data of cubic phase Al (red lines) [21].

For determining the compositions of the Me-C coatings, X-ray Photoelectron Spectroscopy (XPS) was used. This was carried out with a Physical Electronics Quantum 2000 ESCA microprobe instrument, and measurements were carried out both on the surface of the samples and at different depths by etching with Ar^+ ions (1 keV). Besides chemical composition, XPS also gives information regarding chemical bonding that are present for a film, such as Me-O, Me-C and C-C bonds. By determining the bonds present, it is possible to identify what phases are present.

An example of XPS-spectra from both surface (red) and bulk (blue) are shown in figure 4. Here, it is possible to see what was present on the surface and in the bulk of an Al film. Besides Al, only the surface contaminant carbon and oxygen were detected. Worth noting however, is that the presence of O was higher than anticipated (both on surface and in bulk). This is due to that new oxide layers start to form during analysis.

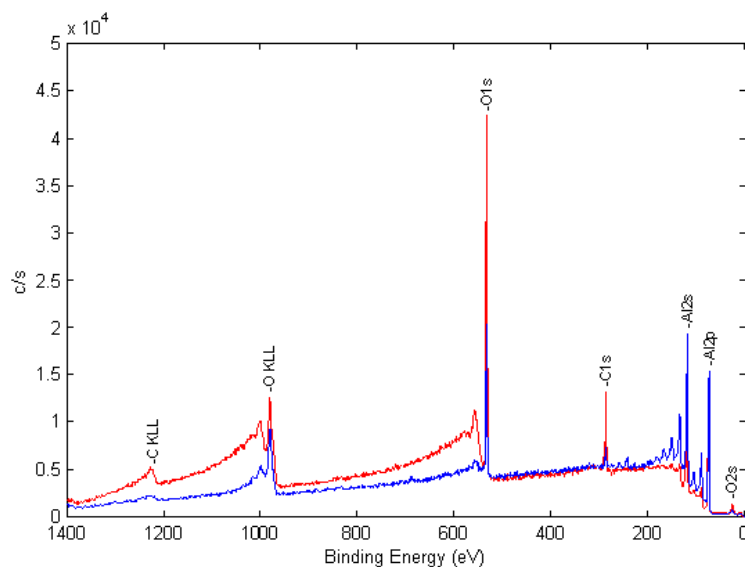


Figure 4 XPS spectra of an Al film (blank). It can be seen that oxygen and carbon mainly exist on the surface (red) and not as much in the bulk (blue).

XPS analysis can also be done at different depths in order to determine what chemical bonding are present at the different depths, see figure 5. For a given XPS peak, it can be seen that the heights of bonding peaks change the deeper the analysis goes. For an Al film, it is seen in (b) that the presence of oxygen is the highest on the surface. Deeper into the bulk, this oxygen peak gets reduced, indicating that the presence of oxygen is becoming smaller. Eventually, it is seen that the presence of oxygen is practically gone when analysis takes place deep enough in the bulk (i.e. the peak is flat). By the same logic, it is seen in (a) that the Al-Al peak is the highest occurring peak deep inside the bulk, and the Al-O peak is reduced. This indicates that only Al-Al bonds are present in the bulk, which is expected.

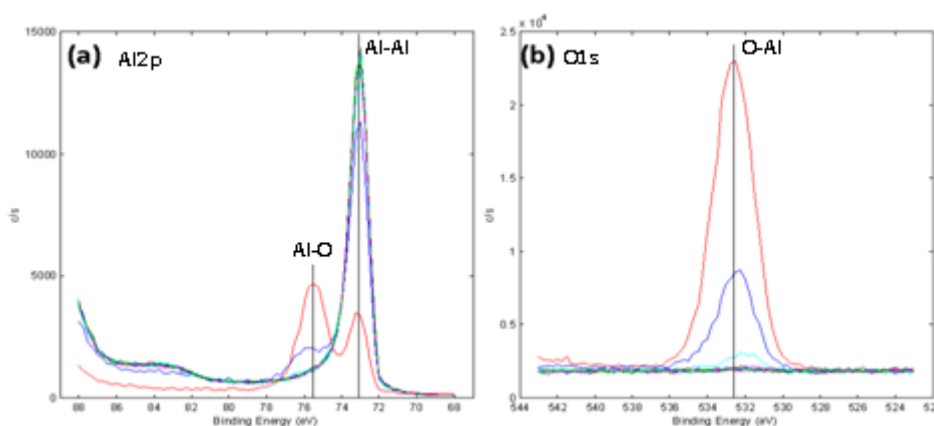


Figure 5 XPS spectra of (a) Al_{2p} and (b) O_{1s} peaks at different depths. Red peaks indicate the surface for each spectral region, and the other colored peaks (which may overlap) indicate other specified bulk depths. In the Al_{2p} region, two different chemical states can be identified: Al-O and Al-Al.

However, since XPS has a low depth of detection (about 10-15 Å for carbides), problems will arise in case of contaminants (Galinstan residues in this case) are present. In this situation, contaminants will “block” the film underneath, which leads to that the film cannot be measured.

2.2. Materials

Al-films were deposited with a power of 1600 W for 1 minute, resulting in 430 nm thick Al-films on top of microscope slides (38x21 mm). MeC_x films were deposited on top of Al films using an unbalanced, non-reactive DC magnetron sputtering in a UVH chamber [18]. In total, 2-4 plates of each MeC_x and Al were produced before the start of the project. These were cut into smaller pieces (19x13 and 13x9 mm) in order to obtain more samples. All samples are presented in table 1. Chromium carbide (CrC), titanium carbide (TiC), niobium carbide (NbC) and zirconium carbide (ZrC) were studied seeing how these were the only available carbides to produce. The CrC films were also sputtered with different compositions (Carbon-rich, C_{rich} and Carbon-poor, C_{poor}) according to the works Andersson *et al.* [18]. Each film was deposited with a pressure of 3.0 mTorr and at different times and temperatures, but all Me-C films were estimated to be ~200 nm thick. The current for Me and C was varied in order to control compositions. A bias of -50 V was used in order to increase coating adherence and reduce porosity. With XRD and XPS analysis of the five Me-C films' blanks, phases and chemical composition with respect to Me, C and O, as well as chemical bonds, were determined. This data is presented in table 1.

Table 1 shows the sputtering parameters used for films, and results of XRD and XPS analysis.

Top coating type	Current Me (mA)	Current C (mA)	Time	T (°C)	Observed phases in XRD	Compositions	Bonds in bulk by XPS	Film phases
						from XPS [Me];[C];[O] (at%)		
Al	---	---	1min	---	Al	99;0;1	Al-Al	Al
CrC _{rich}	27	300	2h 47min	300	Al	37;63;0	Cr-C	a-CrC _x
CrC _{poor}	75	300	1h 51min	300	Al	62;35;2	Cr-C+C-C	a-CrC _x /a-C
TiC	167	250	1h 15min	220	TiC, Al	47;48;5	Ti-C+C-C	nc-TiC/a-C
NbC	150	250	1h 15min	220	NbC, Al	55;40;5	Nb-C	NbC _x
ZrC	150	250	1h 15min	220	ZrC, Al	54;42;4	Zr-C	ZrC _x

XRD analysis showed that all films contained Al, since both the MeC_x and Al films were analyzed. Depending on what film phases that were present, diffractograms would be slightly shifted towards lower 2θ degrees compared to references. Peaks were also broader for the analyzed carbide films. For instance; Ti-C will be shifted towards lower 2θ degrees as it was nanocomposite, which Jansson *et al.* have studied [16]. Peak positions also depend on stoichiometry (NbC_x, ZrC_x): If this was varied, diffractograms can deviate in comparison to references [22].

2.3. Initial experiments

2.3.1. Al films

The method was tested in order to perform successful results in later experiments. Problems immediately appeared with pipetting, as Galinstan adhered to the pipette tip. This problem remained whether the application was done by touching the film or not. This resulted in that Galinstan was applied up to 5 seconds after it was pressed out, and a non-spherical shape of the drop was obtained, see figure 6. The shape of the drop was thinner at the top, whether it was an Al film or an MeC_x film. This was due to the application, since Galinstan adhered to the pipette tip. Once applied, the drop stuck on the Al-plate with no problems.

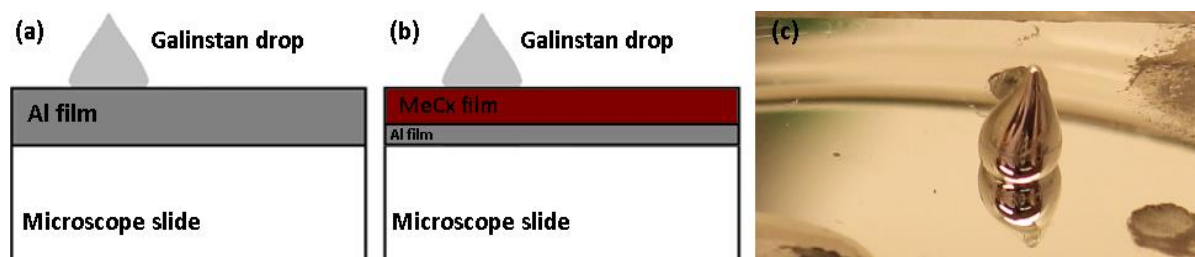


Figure 6 The experimental set-up with (a) a Galinstan drop on top of an Al film, (b) a Galinstan drop on top of an MeC_x film which is on top of an Al film, and (c) shows a photograph from one of the initial experiments with a drop of Galinstan on top of an Al film.

2.3.2. CrC films

A similar experiment as described above for Al was performed with Cr-C films. The two different compositions Cr-C_{rich} and Cr-C_{poor} were tested. Worth noting was that Galinstan adhered far less to these surfaces compared to the Al coating. However, applied drops still sustained a deformed shape due to the strong adhesion towards the pipette tip of the automatic pipette (as seen in figure 6).

2.4. Main experiments

Films were exposed to Galinstan for different amounts of time, see table 2. Blank samples were preserved for all thin films to have references for later analysis. All films without mentioned temperature have been obtained in ambient conditions (i.e. ca 20°C). For example, there are 5 CrC_{rich} films in total, where 1 is blank, 1 is exposed to Galinstan for 7 hours, 1 for 24 hours, 1 for 13 days and 1 for 7 hours at elevated temperatures (150 °C). Fewer times were tested for Al and Cr-C coatings as some samples had been used for initial experiments.

For experiment at elevated temperatures, a furnace heated to 150 °C was used. One of each Me-C films and an Al film were put together in a petri dish. Worth noting was that the furnace temperature dropped from 150 °C to ~140 °C every time the furnace was opened in order to take photographs. Once the time had elapsed, the films were cooled down to room temperature inside the furnace before they were taken out.

Table 2 Experimental test matrix, showing how samples were exposed.

Film type	Galinstan exposure time						
	Blank	7 hours	18 hours	24 hours	7 days	13 days	7 hours 150 °C
Al	x	x	x	x	x		x
CrC _{rich}	x	x		x		x	x
CrC _{poor}	x	x		x		x	x
TiC	x	x	x	x	x	x	x
NbC	x	x	x	x	x	x	x
ZrC	x	x	x	x	x	x	x

Galinstan drops for all experiments were removed by sweeping it off by hand (with glove protection), using a single stroke, in order to be able to examine the film underneath (i.e. the mark left on the film by the Galinstan drop). Although Galinstan was not toxic, glove protection was used to avoid possible contaminations of the samples.

3. Results

3.1. Initial experiments

3.1.1 Al films

When a drop of Galinstan was applied to an Al film, the shape of the drop sustained up to 12 minutes after application, see figure 7. After 12 minutes, the drop started to stabilize its' shape into a more sphere-like form. Once it became more spherical, color-changes could be observed, arising from the top of the Galinstan drop. This color was first rust-like and after awhile it grew to become darker. It was seen that, 30 minutes after application, that the color would not change much further. This indicates that Galinstan in fact reacts with Al.

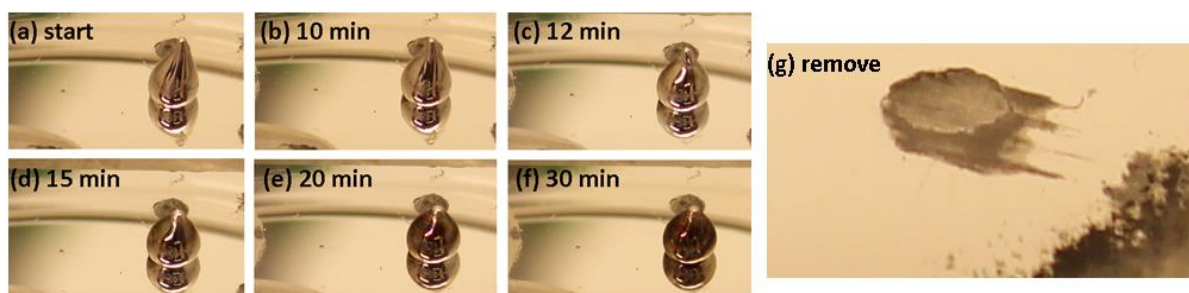


Figure 7 Galinstan drop on Al film photographed during (a) at the start of the experiment, and (b) 10 minutes, (c) 12 minutes, (d) 15 minutes, (e) 20 minutes, (f) 30 minutes after application, (g) shows a zoomed-in photograph of a mark from a removed drop. It was seen in (c) that some color changes have appeared on top of the drop, and in (g) that the drop had corroded through the Al film.

After removing the drops, it was seen that it had corroded through the Al film so that the microscope slide underneath the film was visible. Thus, a reaction taking place between Al and Galinstan could be concluded (i.e. Al is no longer present where the Galinstan drop was). Small residues of Galinstan could be seen where the drop was placed after removal.

3.1.2. Cr-C films

It was observed that for the Cr-C_{rich} plate, Galinstan reacted in less than 3 minutes: Cracks started to form in the carbide film around the drop, as well as color-changes of the drop, see figure 8. This region expanded over the entire plate over time as well as the drop changed in color. This crack formation is taken as evidence for a reaction taking place.



Figure 8 Cr-C_{rich} film with a Galinstan drop. Color-changes of the drop was seen as well as that cracks started to form.

Two hours after application, the cracks had expanded further, see figure 9. What could be seen was that the cracks diverged the further away it spread from the drop, which could be described as gradual color change – The further away the cracks spread from the drop, the “brighter” the color of the cracked region appeared. Furthermore, in a separate experiment, cracks were observed around the drop. However, relocating this drop to a new position would result in no further reaction: The cracks at the old position would not expand further, and the drop would not cause crack formation at the new position. This relocation was done 5 minutes after application, and the drop did not cause any new reaction after 2 hours at this new position. This hints that Galinstan diffuses into the film rapidly, seeing how cracks start to spread from where the drop was applied. If Galinstan was removed from where cracks started to form, the diffusion rate would decrease. This was expected, since then there would be “nothing that could diffuse into the film” if Galinstan was removed. However, the exact diffusion mechanism of Galinstan is unclear, though it is believed that the diffusion is initiated depending on how Galinstan was applied.

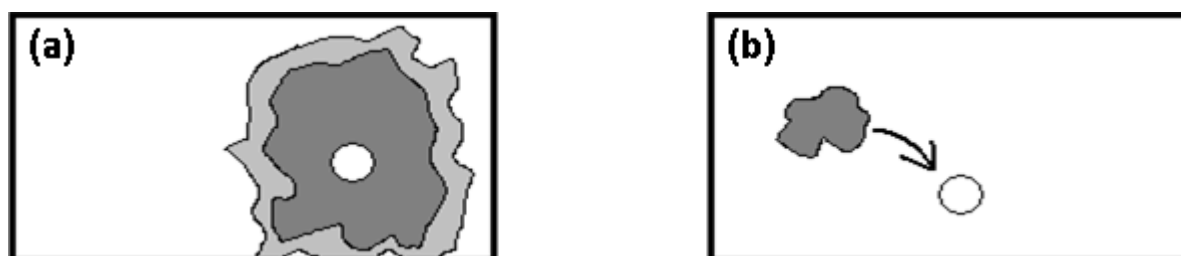


Figure 9 Sketches showing results of initial experiments on Cr-C_{rich} coating. (a) A Galinstan drop that was applied on a Cr-C_{rich} film after two hours, showing different cracked regions. (b) Relocating the drop did not cause any crack formation at the new position.

To the completely cracked coatings, additional drops were applied. This did not cause any further reaction, as indicated by no change in drop color nor film cracking. They were held over longer periods of time without any reactions occurring. This is taken as evidence that the reaction has reached equilibrium (i.e. the reaction has ended).

Since cracks started to form around the Galinstan drop on the Cr-C_{rich} film, it was tested whether or not the pipetting method caused this to happen. By scratching an already-applied, non-reacted drop on any Cr-C film using a pipette tip, it could be seen immediately that cracks started to form. Also, application of a drop by touching the plate was tested, which resulted in the same reactions taking place. Another test involved scratching a Cr-C_{rich} film before applying Galinstan. Galinstan was applied to the scratched film 2 hours after scratching, and crack formation as described above occurred.

By applying the drop on the film without touching it, no reaction was observed. This led to the conclusion that application of Galinstan drops needs to be done without touching the films with the pipette in further experiments. However, this conclusion still needs to be confirmed with further analysis. It has not been noted if all reactions thus far were due to the pipette touching the films, hence analysis of scratched films in comparison to unscratched films is required. Such analysis will be taken into account in section 3.7. *Scratching with pipette.*

Similar experiments were carried out with the Cr-C_{poor} film. It could be seen that Galinstan would not react with the film – cracks around the Galinstan drop could not be seen after removal. In fact, drops barely adhered to the Cr-C_{poor} film, resulting in that drops could easily ‘roll off’ of the film through e.g. tilting.

3.2. Al films

The Al films used for the main experiments reacted similarly to what was described in section 3.1.1. *Al films*: The Galinstan drop would sustain its’ shape up to 12 minutes after application, at which it would change shape and become darker. However, in some cases, it was observed that this reaction would occur much later (up to 40 minutes until the drop’s shape started to change), if at all. One case where a Galinstan drop was applied on an Al film, no reaction was observed, see figure 10. This drop was held for 24 hours on the Al film and nothing ever happened during the elapsed time.

After removal of the drop by sweeping it off with glove-protected hands, a mark was found underneath, whether the drop changed shape or not, thus indicating a reaction in all cases. Just as seen in section 3.1.1. *Al films*, the drops had corroded the film so that the microscope slide underneath was visible. This behavior was also present for an Al film which was exposed to Galinstan for 7 days.

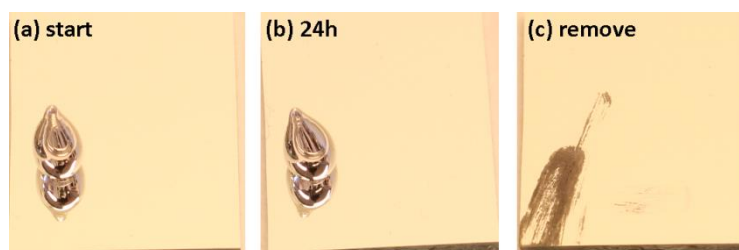


Figure 10 Al film photographed at (a) start of the experiment, (b) 24 hours later and (c) after removal.

The temperature experiment yielded some interesting observation when it came to the Al film. During the time of 10 minutes after the film was inserted in the furnace, a non-reacted (i.e. no shape or color changes) Galinstan drop had ‘melted’ on top of the film, see figure 11. This condition remained throughout the whole temperature experiment (with slight changes in shape) until it was pulled out of the furnace and remained in ambient conditions for 5 minutes. At this point, the Galinstan ‘melt’ had corroded the entire film and turned darker in color. Upon removal of the ‘melt’, the entire film was swept off. These observations suggest that the presence of water (humidity) is needed for the reaction, as water cannot condense in the furnace due to the temperature of 150 °C.

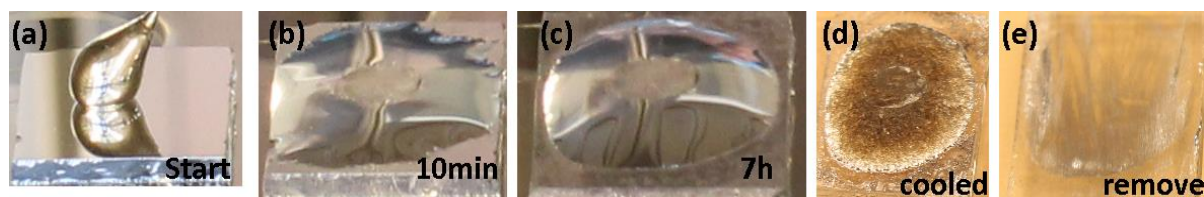


Figure 11 Photograph series of an Al film and Galinstan drop in elevated temperatures at (a) start, (b) 10 minutes, (c) 7 hours after application, (d) 5 minutes after the film was taken out from the furnace and (e) after removal of ‘melt’.

XRD analysis yielded no difference between the unexposed and exposed films, see figure 12. Only the cubic structure of Al was observed [21]. This is expected, since Galinstan had only corroded the Al film without leaving any noticeable changes to the surface. Thus, the diffractograms of the two films will look similar.

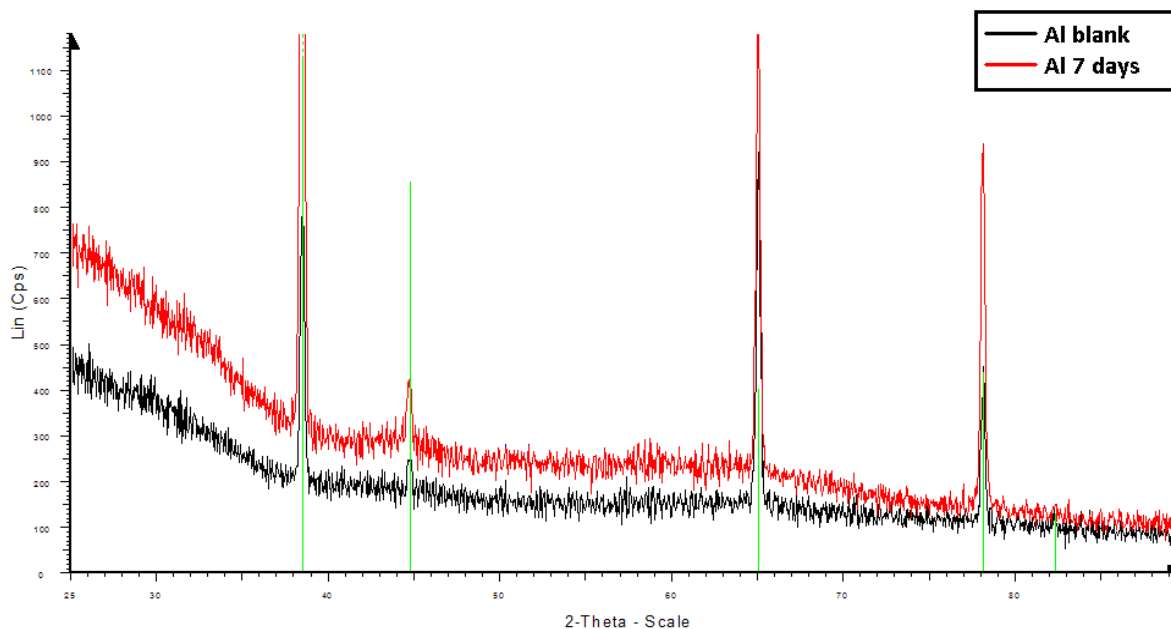


Figure 12 Diffractogram of an Al blank (black) and an Al film which was exposed to Galinstan for 13 days (red) with reference of fcc Al (green lines) [21].

No XPS analysis was carried out for any reacted Al films. This was due to that the marks that Galinstan had left behind consisted of no Al, due to Galinstan corroded through, resulting in exposing the underneath microscope slide).

3.3. Cr-C films

3.3.1. Cr-C_{rich} films

Out of three CrC_{rich} films, one reacted within 2 minutes after application of Galinstan, see figure 13. The drop started to change color and cracks started to form around the drop that expanded over time (as described in section 3.1.2. *Cr-C films*) and the experiment was cancelled 24 hours after application. The other two films never reacted, even though these films were held for over a week. This strongly indicates that the reacted sample must have been affected in one way or another, e.g. from how the Galinstan drop was applied on the film. Removing the drop of the reacted film left residues of Galinstan, as seen in (f) in figure 13. It was not possible to see through the mark (i.e. if the microscope slide underneath was visible) because of the residues.

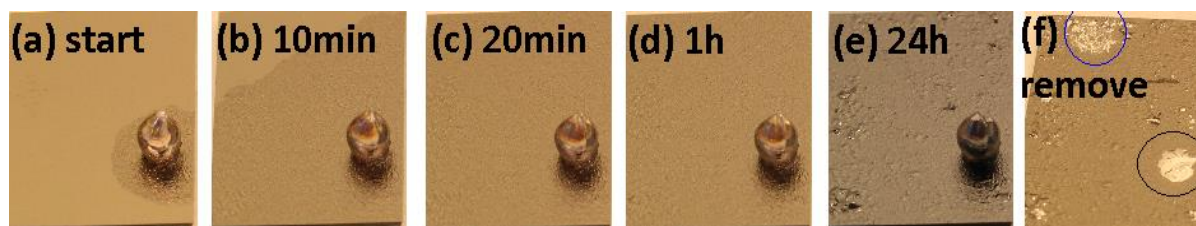


Figure 13 Cr-C_{rich} film photographed at (a) start of experiment, (b) 10 minutes, (c) 20 minutes, (d) 1 hour, (e) 24 hours after application, and (f) after removal. In (f), residues could be seen where the drop was (black circle) and at the top of the film (blue circle, due to Galinstan accidentally scattered to this location). Photograph (e) is dark due to the lights were unintently turned off during photographing.

As for the non-reacted films, only the film which was exposed to Galinstan for 13 days had left a bright mark consisting of residues where the drop was. Also, the sample exposed to 150°C showed the same mark, see figure 14. The reaction is evidently time-controlled, but the reaction rate increases with temperature.

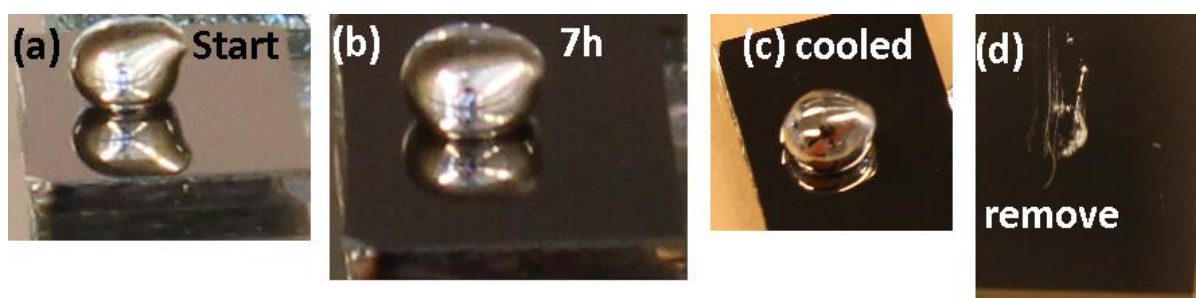


Figure 14 Photograph series of a Cr-C_{rich} film exposed to Galinstan at elevated temperatures, at (a) start of the experiment, (b) 7 hours after application of Galinstan, (c) after cooling the sample and (d) after removal.

From XRD analysis, it can be seen that Galinstan would not cause any change of the film structure by comparing diffractograms from the unexposed and exposed samples, see figure 15. Since the Cr-C_{rich} films were amorphous (a-CrC_x, see section 2.2. *Materials*), it is expected that no CrC references [23,24] would match the diffractograms. However, Al appears in both cases [21]. Therefore, Galinstan did not affect the crystal structure of the Cr-C_{rich} film.

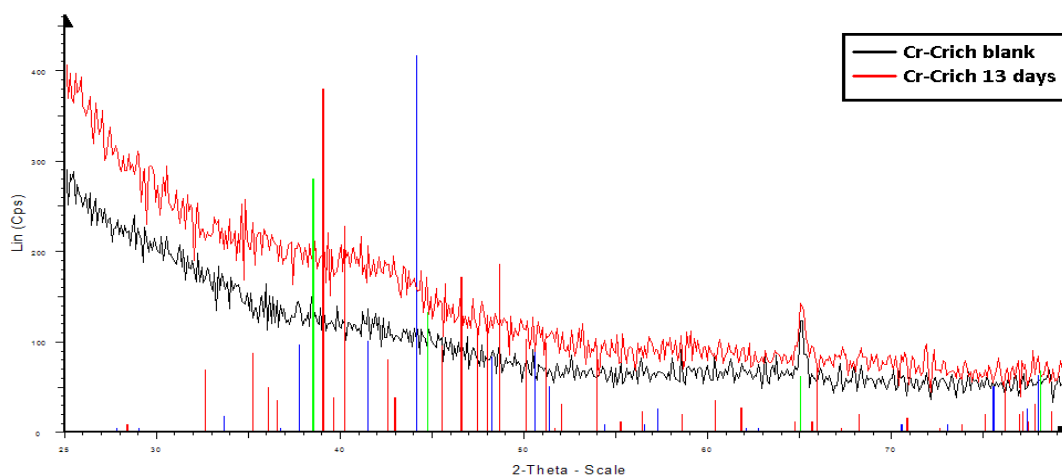


Figure 15 Diffractogram of Cr-C_{rich} blank (black) and sample which was exposed to Galinstan for 13 days (red). It was seen that no CrC references (Orthorhombic, red lines; cubic, blue lines) matched any peaks, but Al (green lines) did [21,23,24].

However, the sample which had reacted within 3 minutes was analyzed and its' diffractogram looked different compared to the Cr-C_{rich} blank, see figure 16. When compared to Ga, In and Sn references [25,26,27], and it can be seen that the very broad features may stem from very small (a few nanometers) Ga-crystallites (Ga reference lines in blue), which would give very broad diffraction features.

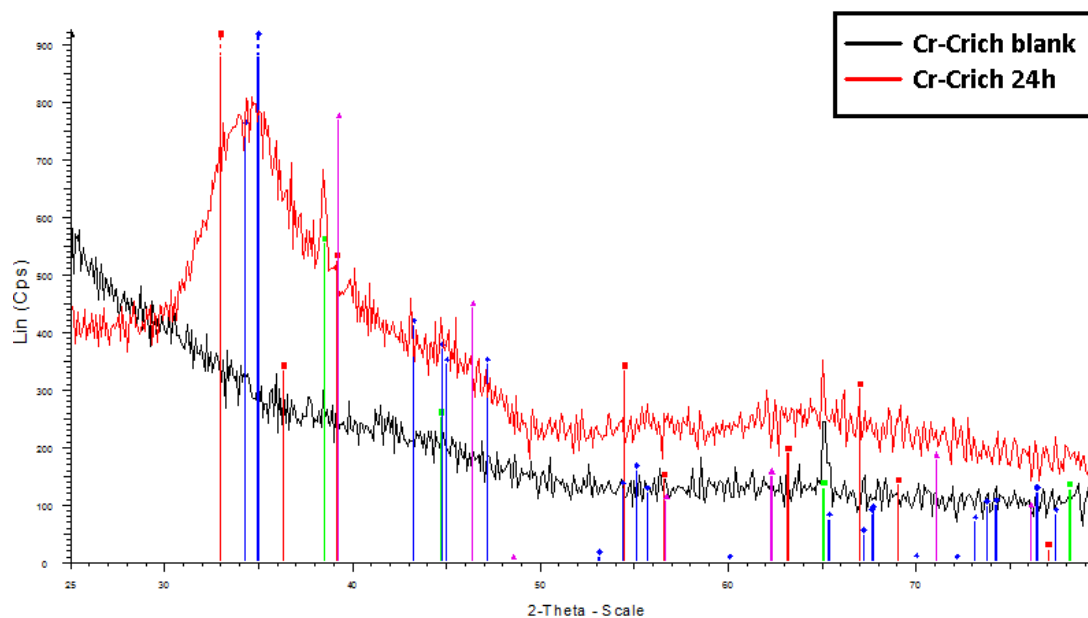


Figure 16 Diffractogram of Cr-C_{rich} blank (black) and 24 hours reacted sample (red). Al (green lines), Ga (blue lines), In (red lines) and Sn (pink lines) references were added [21, 25, 26, 27].

XPS analysis was carried out on the Cr-C_{rich} film which was exposed for 13 days. It was measured at different positions of the film: On the mark where the drop was, in a cracked region and on nearby Galinstan residues, see figure 17. By comparing each XPS spectrum, it was seen that Ga, In and Sn regions increased from (a) to (d) and that Cr peaks were seen. Due to the surface sensitive nature of XPS, this indicates that Galinstan “blocks the film” for analysis. Also worth noting is that no Al peaks were observed, indicating that Galinstan had not penetrated through the Cr-C_{rich} film.

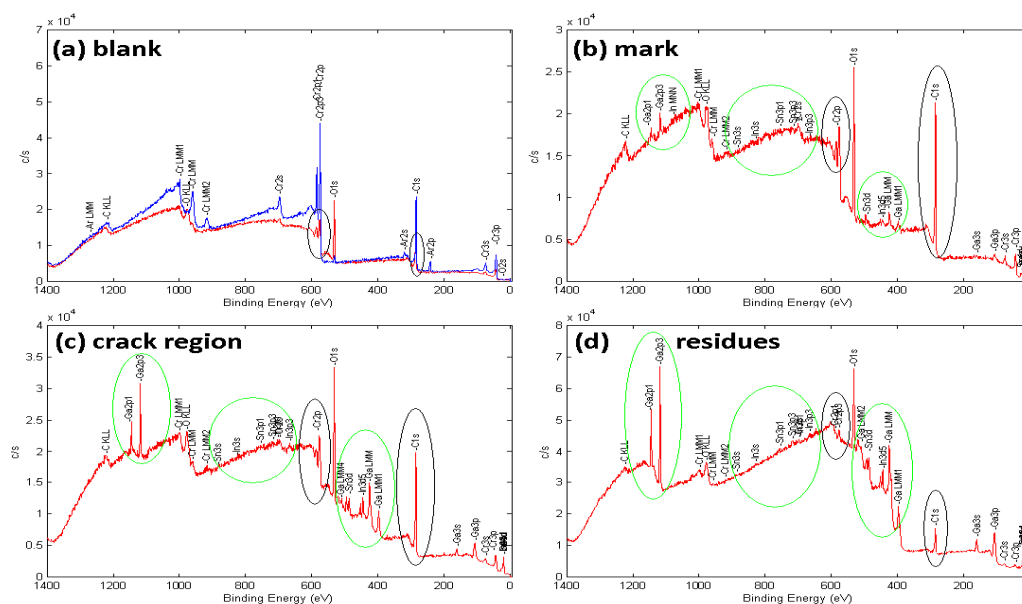


Figure 17 spectra of the Cr-C_{rich} which was exposed to Galinstan for 13 days at (a) blank sample, (b) mark of Galinstan drop, (c) crack region around the mark and (d) Galinstan residues present on the sample. Black and green circles show Cr and C peaks and Ga, In, Sn regions, respectively.

3.3.2. Cr-C_{poor} films

For all Cr-C_{poor} films, no reactions occurred in 13 days, see figure 18. This agrees with the initial experiments seen in section 3.1.2. *CrC films*. Drops of Galinstan, for all CrC_{poor} films, barely adhered so that drops could be removed by e.g. tilting the sample.

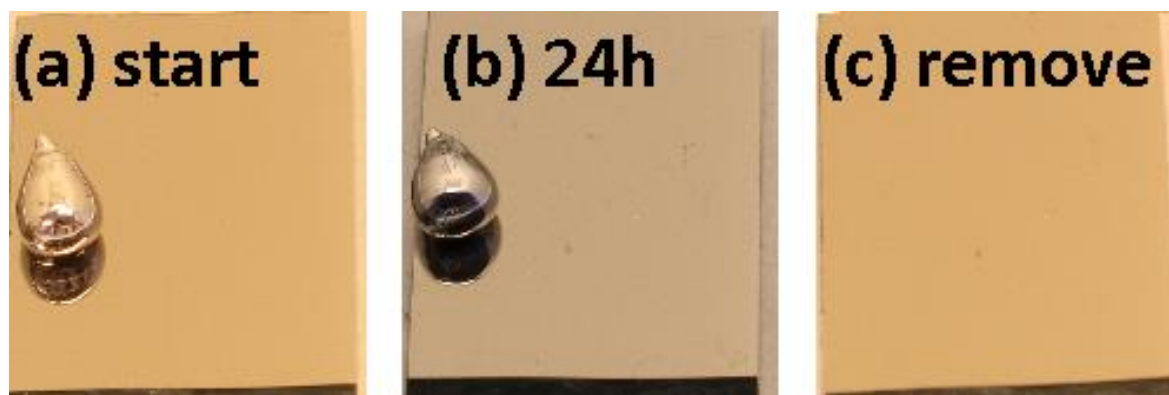


Figure 18 Cr-C_{poor} film photographed at (a) start of experiment, (b) 24 hours after application of Galinstan drop and (c) after removal. Photograph (b) is dark due to the lights were unintendedly turned off during photographing.

Also, it appeared that no reactions occurred for temperature experiments of the Cr-C_{poor} film, see figure 19. Once again, drops were easily removed by tilting the film.

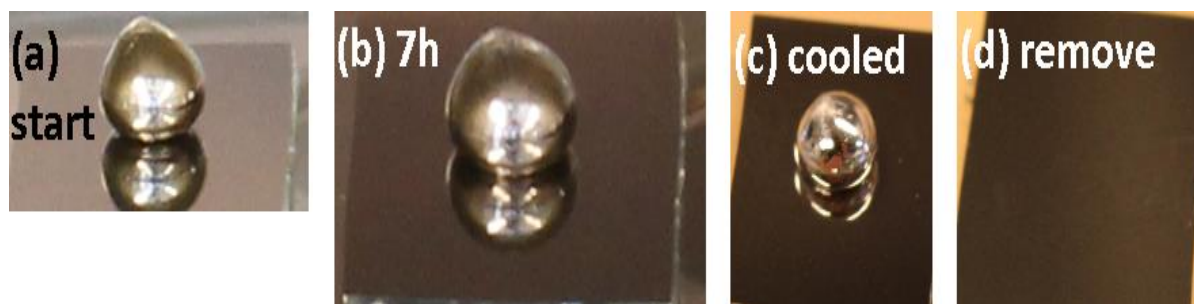


Figure 19 Photograph series of a Cr-C_{poor} at elevated temperatures at (a) start of the experiment, (b) 7 hours after application, (c) after cooling the sample and (d) after removal.

No marks were left on the films after removing the drops. XRD analysis also showed no difference between the unexposed and exposed films, see figure 20. No obvious changes could be seen between the samples, as well as no references more than Al matched obvious peaks [21,23,24]. Therefore, Galinstan did not affect the structure of the Cr-C_{poor} film either. Since no reaction occurred, XPS analysis was not carried out – there was nothing to examine, after all.

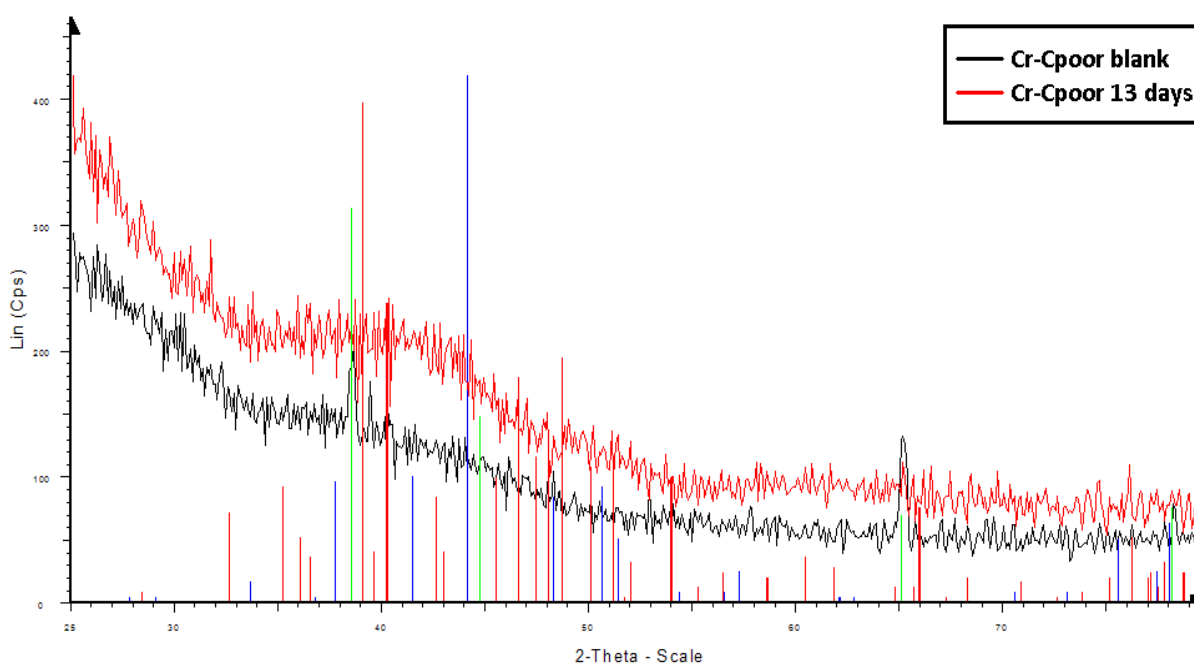


Figure 20 Diffractogram of Cr-C_{poor} blank (black) and Cr-C_{poor} film that was exposed to Galinstan for 13 days (red). Orthorhombic CrC (red lines) and cubic CrC (blue lines) references did not match any peaks, though Al (green lines) reference did [21,23,24].

3.4. Ti-C films

It was seen that Ti-C films showed low reactivity towards Galinstan. After one hour, no change of any Ti-C films were observed: No change of the drop shape nor any changes on the film. Also, after 24 hours no signs of reaction were observed, see figure 21. However, removing the drops initiated a reaction on the films, seemingly due to the remaining residues of Galinstan. The films started to crack up, expanding across the film along with the direction the drops were swept off. However, the cracks stopped expanding after 10 minutes. Initially, marks could not be seen underneath the films after the drops were removed. It was only noticeable once crack formation started to take place. The same observations were made for a film that was exposed to Galinstan for 13 days. These observations suggest that Galinstan only reacts with Ti-C if the film surface was scratched upon removal, as it would not react otherwise.



Figure 21 Ti-C film photographed at (a) start of the experiment, (b) 24 hours later and (c) after removal.

In the temperature experiment, the drop sustained the same form on the film during the whole time. Furthermore, no reaction could be seen on the film itself. Only after removing the drop by sweeping it off would something happen, see figure 22. Similar crack formation as seen in the room temperature experiments were observed upon removal. The difference was that these cracks spread wider over the film.



Figure 22 Ti-C film in elevated temperatures at (a) start, (b) 7 hours after application, (c) 5 minutes after the film was pulled out from the furnace and (d) after removal.

From XRD analysis, it was seen that the crystal structure of the Ti-C film had not changed upon exposing it for 13 days to Galinstan, see figure 23. Ti-C peaks are slightly shifted towards lower 2θ degrees and appeared wider compared to references [28]. This was expected, as Ti-C films had a nanocomposite structure (see section 2.2. *Materials*) [16].

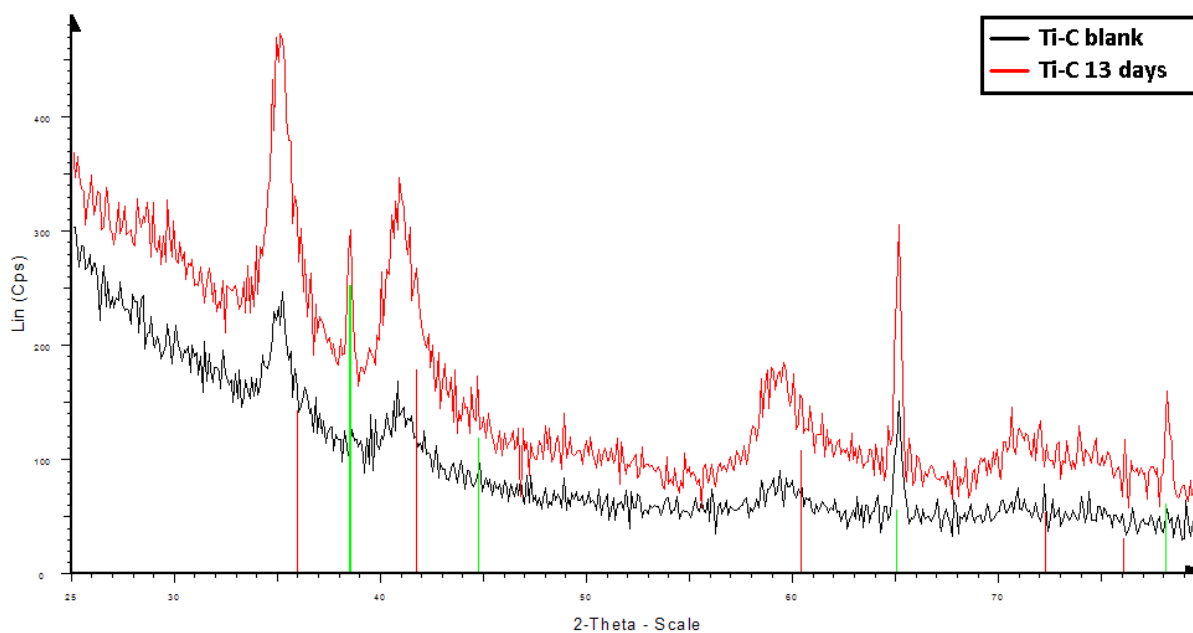


Figure 23 Diffractograms of Ti-C blank (black) and a Ti-C film which was exposed to Galinstan for 13 days (red). Both diffractograms are slightly shifted compared to Ti-C references (red lines), but align well with Al references (green lines) [21,28].

From XPS analysis of the blank and 13 days Ti-C films, it was seen that Al is observed at the reaction mark from Galinstan exposure, see figure 24. By comparing the two spectra, the Ti peaks were not detected and Al peaks had appeared for the exposed Ti-C film. This would indicate that Galinstan in fact has penetrated through the film and reacted with the available Al.

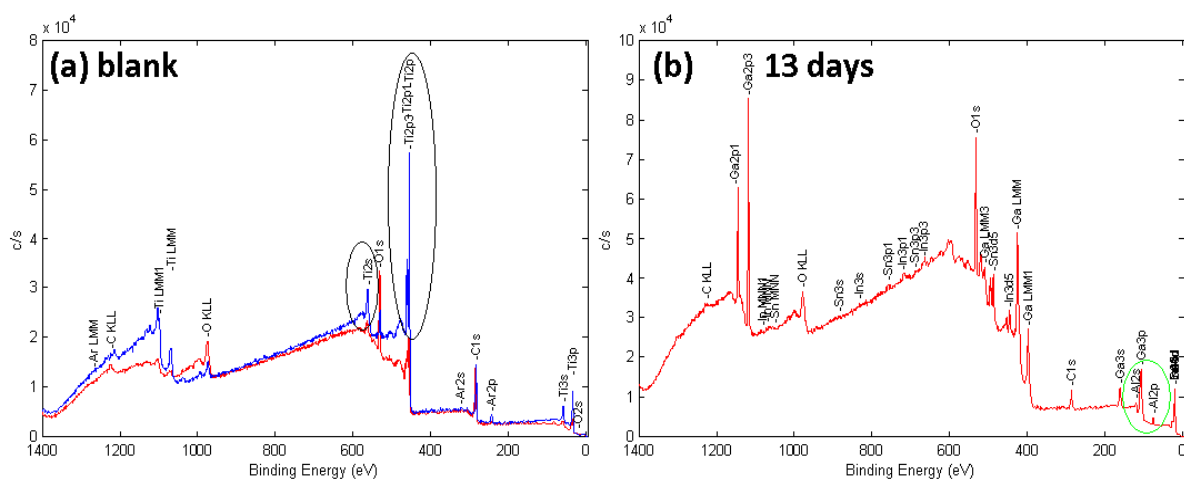


Figure 24 XPS spectra of (a) blank Ti-C film and (b) Ti-C film which was exposed for 13 days (on the mark of the film, see figure 21(c)). Red spectra indicate surface analysis and blue represent bulk. Ti and Al peaks are marked with black and green circles respectively.

3.5. Nb-C films

Experiments of Nb-C films yielded quite similar results to those of Ti-C, see section 3.4. *Ti-C films*. That is, no reactions occurred for 24 hours, nor did the shape of the Galinstan drop change over time, see figure 25. Also, cracks would start to form along the direction in which the drop was swept off upon removal, and would stop expanding after 10 minutes. No marks could be seen underneath the film after removing the drop, until cracks started to appear. The same was seen with a film which was exposed to Galinstan for 13 days. Just as in the case of Ti-C, these observations suggest that Nb-C films would only react in case the film surfaces were scratched.



Figure 25 Nb-C film photographed at (a) start of the experiment, (b) 24 hours later and (c) after removal.

Similarly to Ti-C, the Nb-C film did not react during the temperature experiment: Both the shape of the drop and the Nb-C film itself did not change. It was only when the drop was removed by sweeping it off that reactions started to occur (crack formation), see figure 26.

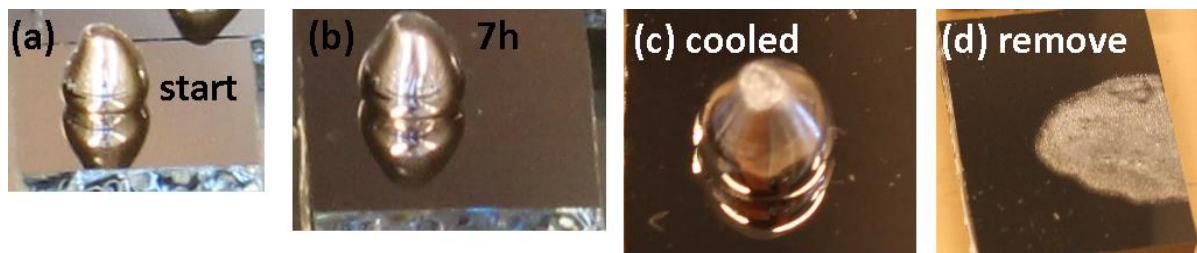


Figure 26 Nb-C film in elevated temperatures at (a) start, (b) 7 hours after application, (c) 5 minutes after the film was pulled out from the furnace and (d) after removal.

From XRD it was seen that the crystal structure of Nb-C was unchanged upon exposure of Galinstan in 13 days, see figure 27. The diffraction peaks were slightly shifted towards lower 2θ degrees compared to reference values [29], for both samples.

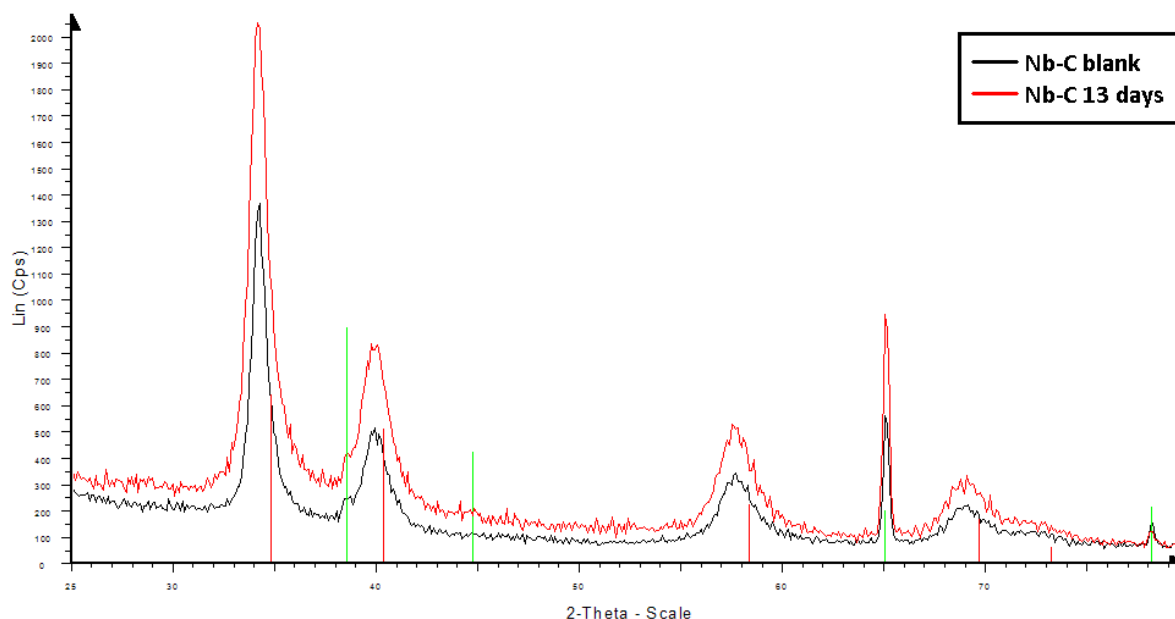


Figure 27 Diffractogram of Nb-C blank (black) and Nb-C film exposed for 13 days (red). Peaks are slightly shifted towards lower 2θ degrees compared to Nb-C references (red lines), while Al agrees with Al references (green lines) [21,29].

XPS analysis also showed similar results as the Ti-C analysis, seen in section 3.4. *Ti-C films*. Al was detected on the Nb-C film that was exposed to Galinstan for 13 days, see figure 28. By comparing XPS spectra of the Nb-C blank and the Nb-C film that was exposed for 13 days, the Nb peaks in the latter spectrum have almost vanished. Just like the Ti-C films discussed in section 3.4. *Ti-C films*, it was seen that the Nb-C film have been penetrated by Galinstan and reacted with the Al film underneath.

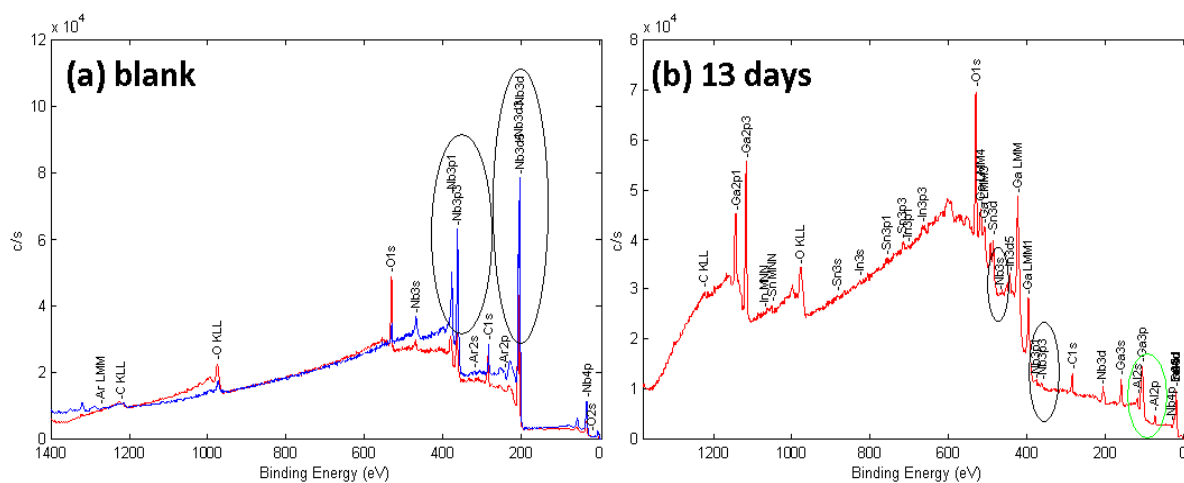


Figure 28 XPS spectra of (a) blank Nb-C film and (b) Nb-C film which was exposed for 13 days (on the mark). Red and blue spectra correspond to surface and bulk analysis respectively. Black circles are drawn to indicate Nb and green circles indicate Al.

3.6. Zr-C films

For all Zr-C samples, no reaction seemed to take place during 24 hours of exposure to Galinstan, see figure 29. Unlike the case of the Ti-C and Nb-C films, the Zr-C film never formed any cracks after removing the Galinstan drop for all experiments (including the temperature experiment). Instead, a small, circle-like mark of Galinstan residues was seen on the film where the drop had been. It remained so for more than 10 minutes, until some cracks could be seen in the direction which the drop was swept off. This was only seen for the Zr-C film which was exposed to Galinstan for 13 days. Unlike the Ti-C and Nb-C films, no marks could ever be seen underneath the Zr-C film. This indicates that Galinstan does not penetrate the ZrC film, and is thus unable to react with the Al film underneath.

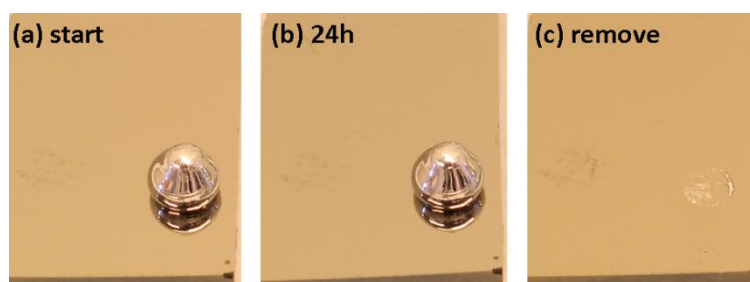


Figure 29 Zr-C film photographed at (a) start of the experiment, (b) 24 hours later and (c) after removal.

As for the temperature experiment, the Zr-C film remained non-reacted throughout the whole experiment, as well as the Galinstan drop remained its' shape, see figure 30. Removing the drop resulted in similar observation as above. This time however, more cracks appeared along the direction the drop was swept off than seen from experiments done in ambient conditions. It also had less Galinstan residues present.

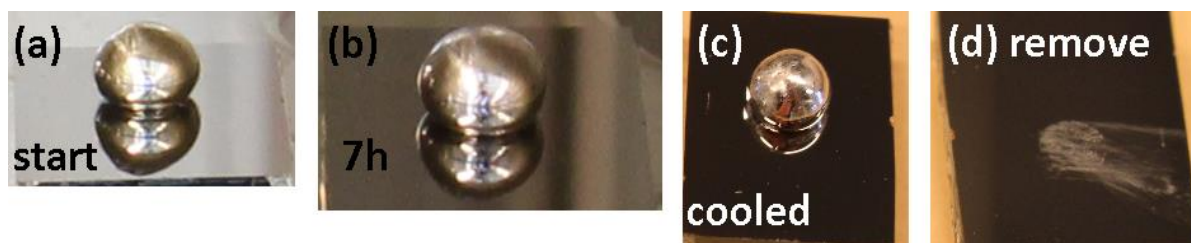


Figure 30 Zr-C film in elevated temperatures at (a) start, (b) 7 hours after application, (c) 5 minutes after the film was pulled out from the furnace and (d) after removal.

XRD analysis showed no differences between unexposed and exposed Zr-C films, meaning that the crystal structure had not changed by Galinstan exposure, see figure 31. Just like the diffractograms for Nb-C (see section 3.5. *Nb-C films*), the diffractograms of Zr-C were also shifted towards lower 2θ degrees compared to reference values [30].

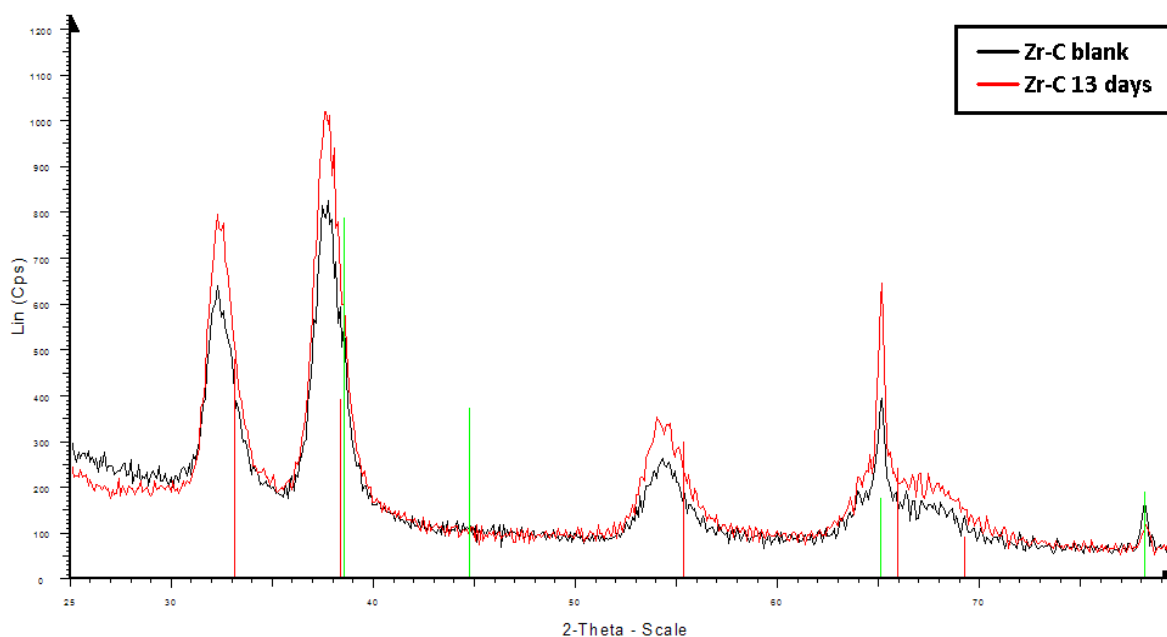


Figure 31 Diffractogram of Zr-C blank (black) and a Zr-C film exposed to Galinstan for 13 days (red). References of ZrC (red lines) and Al (green lines) are shown [21,30].

XPS analysis provided that unlike the Ti-C and Nb-C films, that no Al peaks appeared, see figure 32. This indicated that Galinstan did not penetrate through the Zr-C film, even though the film was exposed to Galinstan for 13 days. However, the Zr peaks have been reduced upon applying Galinstan. As stated in section 2.2. *Materials*, this is due to that residues “blocked the film”, resulting in that the Zr peaks became smaller.

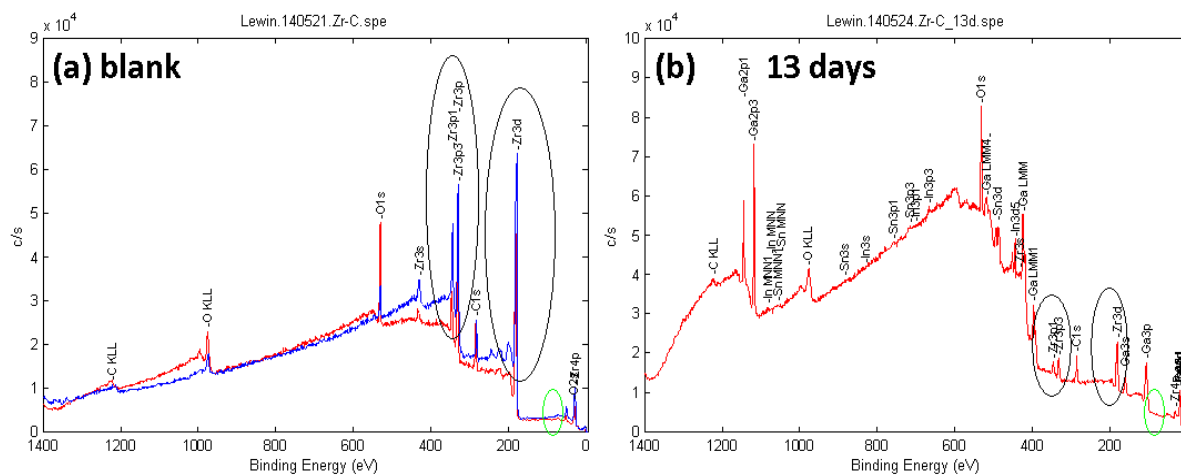


Figure 32 XPS spectrum of (a) Zr-C blank and (b) Zr-C film exposed to Galinstan for 13 days (on the mark). Red and blue spectra are surface and bulk analysis respectively. Black circles indicate Zr peaks and green circles where Al would appear if the Zr-C film was penetrated.

3.7. Scratching with pipette

To test the influence of touching the sample with the pipette tip before exposure to Galinstan, additional experiments were performed. A part of a Ti-C film was scratched with a plastic pipette tip and analyzed with XPS in comparison to an unscratched part of the same Ti-C film to conclude whether scratching the surface of the film would cause any chemical changes or not. It appeared that, in fact, no substantial chemical changes would occur upon scratching the Ti-C film. This was concluded from XPS analysis, see figure 33. It can be seen that the spectra of both the scratched and unscratched films look very alike among them (i.e. (a) and (c) look alike and (b) and (d) look alike). The only difference was that the C-C peak is slightly larger for the scratched film than the unscratched on the surfaces. This may be due to that the pipette was made of plastic, hence “applying” C onto the film surface by scratching.

Essential is the observation that the O peaks (i.e. Ti-O) remained practically the same in both cases. The Ti peaks (i.e. Ti-C for all (a), (b), (c) and (d)) also remained unchanged. This lead to the conclusion that scratching the surface did not affect the surface chemically and the surface oxide of the sample remained intact. Hence, a mechanical change (e.g. producing cracks through the carbide coatings, thus exposing the Al underneath to any Galinstan placed on the sample) must be the cause of increased reactivity upon scratching. In other words, in order to obtain reproducible results it was of necessity not to touch the film upon applying Galinstan.

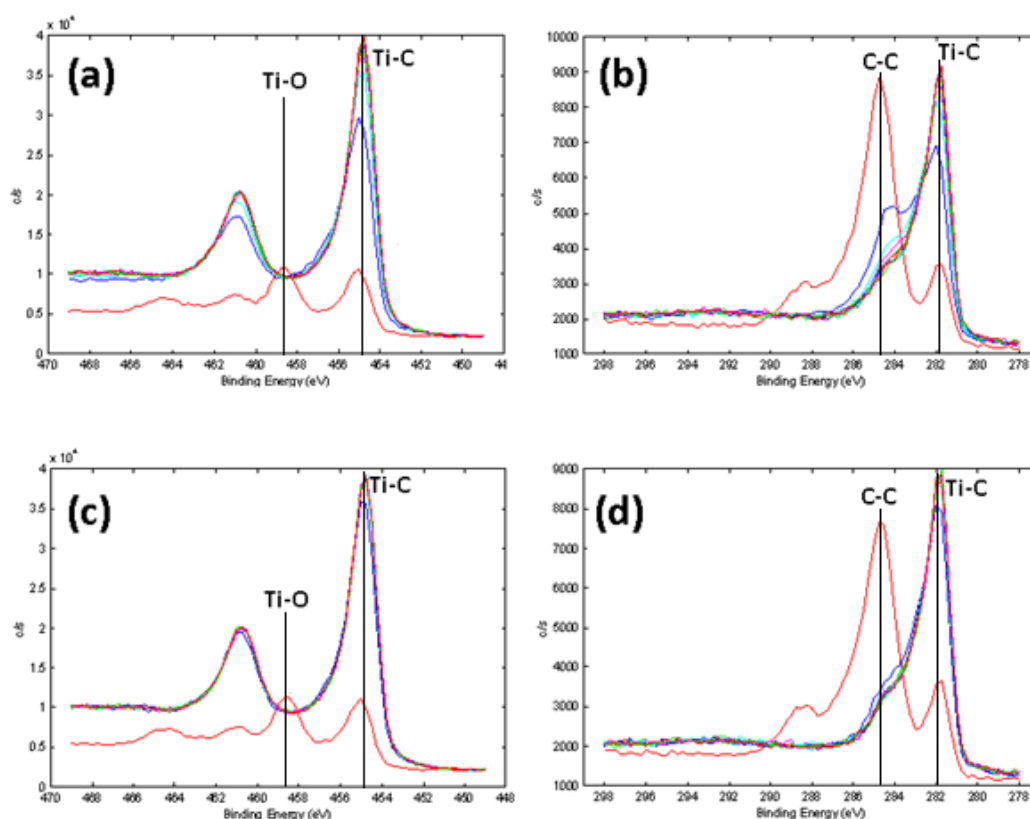


Figure 33 XPS spectra of (a) scratched Ti peaks, (b) scratched C peaks, (c) unscratched Ti peaks and (d) unscratched C peaks. Each peak have been marked with black lines and entitled with corresponding bond types. Red spectra correspond to surface analysis and blue for bulk.

4. Discussion and summary

Throughout the project, it was seen that the observed reactions suggested for some sort of mechanical damages. The following is a list of observations which indicated that mechanical damages may be the cause of initiating corrosion:

- Whether the film surface is touched with the pipette tip upon applying Galinstan or not will determine reaction outcomes.
- By scratching an already-applied drop of Galinstan on a Cr-C_{rich} film, reaction occurred.
- Applying Galinstan onto an already-scratched surface will induce reaction to take place.
- If a drop of Galinstan has reacted somewhere on the film and if it is relocated to another position, it will not react at this new position.
- By removing the Galinstan drops by sweeping them by hand off will lead to reactions occurring afterwards (except for the Cr-C_{poor} films). This will happen whether the drops had reacted before removal or not.

To study the cause of reactions, XPS analysis was employed. It was shown that the oxide layer was not harmed by scratching the MeC_x film with a pipette tip and that the carbon contamination on the surface was minimal. Thus, it can be concluded that chemical reactions occurring upon scratching the film can be excluded. Therefore, further studies must be taken into account in order to determine what specific mechanism that take place upon e.g. scratching the carbide films. Scanning Electron Microscopy (SEM)¹ can be applied in order to study the surface of a scratched and non-scratched MeC_x film.

Related to the described observations of reactions stated above is the question of what kind of reaction that occurs. The following corrosion reactions can be seen visually:

- Cracks start to form upon removal of Galinstan drops by sweeping them off by hand.
- For the Al film, the substrate underneath (microscope slide) is exposed after removing the Galinstan drop.

Chemical analysis of the cracks was applied with XPS. Two important results from this analysis were received:

- In the corroded regions (cracks), Ga, In and Sn were the most observed elements (i.e. Galinstan) in a sense which would be explained with that Galinstan remains on top of the analyzed film.
- Al would be present at this region, but not Me, which means that Galinstan has reacted with Al and not with MeC_x.

This would conclude that Al reacts with the applied Galinstan (it “dissolves” into Galinstan, hence the color changes), but not with MeC_x. The crack formations could therefore be explained with that the “soft” and easily deformed Al film underneath reacts with Galinstan.

¹ For more information regarding SEM, see A.R. West, Basic Solid State Chemistry, 2nd ed., John Wiley & Sons Ltd., 2012, chapter 4

This leads to that Al either loses or changes its' shape, resulting in the hard, yet brittle MeC_x film to fissure.

It was observed that the reaction between Galinstan and Al requires water (humidity). At ambient conditions, water would condense to the sample. This would allow reaction (1) below to occur:



The above reaction suggests that the available Ga₂O₃ from Galinstan (gallium oxide from the surface of Galinstan, see section 1.2. *Galinstan*) reacts with Al. The reduction of Ga is believed to be enhanced by the presence of water rather than oxygen. This could be due to that the bond enthalpies of the O–H single bonds in water is slightly lower than that of the O=O double bond in oxygen (463 and 498 kJ/mol, respectively) [31]. Furthermore, water is also a dipolar molecule with its' two lone pairs, which could be significant for reaction (1) to occur. The true mechanism of the entire reaction is unknown however, which is important to study further. In case if water cannot condense to the sample, the reaction between Galinstan and Al would not occur as easily. Since the Al film in the furnace (i.e. water could not condense to the sample) did not react until the sample was taken out would indicate that water in fact affects the reaction between Al and Galinstan (as water would condense to the sample at this point). It is therefore suggested that water needs to be avoided to prevent reaction to occur.

It was shown with XPS analysis that Al reacted with Galinstan in case cracks on the film were present. The possible reason as to why Galinstan reacts with Al and not with the MeC_x film could be explained with mechanical damages. By scratching (with pipette tip or by hand) the surface of the MeC_x film gets cracked, allowing Galinstan to seep through the MeC_x film and reach Al. Upon scratching, the Al film underneath becomes deformed while the hard MeC_x film stays intact. It may be a disadvantage for the MeC_x films to be hard in this case, as these films will fissure upon scratching. The same can be explained with an Al film (no MeC_x on top). In this case, the oxide layer consisting of Al₂O₃, which is naturally obtained in ambient air, would act similarly as the MeC_x would. Al₂O₃ is, like other ceramics, hard and brittle [32], which makes it comparable with MeC_x in this model. This model needs to be confirmed with further studies, and SEM would once again be a good choice for studying the surfaces.

When it comes to the MeC_x films, the following observations were made:

- Galinstan drops has a low adhesion towards Cr-C_{poor} films. Drops barely adhered so that they could roll off the film by tilting it.
- Neither Cr-C films nor Zr-C films showed signs of corrosion, in case they were not scratched.
- Ti-C and Nb-C films were corroded by Galinstan whether or not the surface was scratched.

The adhesion of the Galinstan drop is very dependent on the surface chemistry, which depends on the transition metal. Another depending factor may be the surface morphology,

meaning how the surface appears on the micro or nanometer scale. Amorphous Cr-C surfaces will have a somewhat smoother surface compared to the crystalline counterpart, which is because amorphous solids lack crystalline grains. Further studies including SEM analysis as well as literature studies should be employed in order to verify this hypothesis.

When it comes to the MeC_x films, the most relevant factors that leads to corrosion of the films are what kind of carbide (i.e. transition metal), microstructure (crystalline, nanocomposite or amorphous), presence of a-C phase and hardness (or rather, brittleness). However, the examined MeC_x films vary too much in these aspects (i.e. different microstructures, presence of a-C differs) in comparison to each other, so no clear conclusion can be made by comparing. A very interesting observation though is that the $\text{Cr-C}_{\text{poor}}$ film has a higher Me composition (highest among all MeC_x films, see table 1 in section 2.2. *Materials*), which will result in a lower hardness [18]. If this is the case, then it agrees well with the model about the flexibility of the MeC_x film causing the Al film underneath to react with Galinstan upon scratching the surface. With hardness measurements, it can be confirmed whether it is the hardness of the MeC_x film that results in the different observations between the Ti-C, Nb-C and Zr-C films.

Overall, the experiments done have shown some interesting results that need to be further studied. However, it could have been performed differently. For instance, the crack formation (diffusion of Galinstan in the film) could be studied closer by recording the process instead of photographing it. The color-change of the drops upon reaction could be studied in such manner as well. Furthermore, studies regarding Galinstan– MeC_x application would be interesting, such as testing the reactivity of Galinstan with MeC_x films with applied electric current or electromagnetic field. This is interesting because this study cannot propose a clear application for Galinstan and MeC_x films, more than that the MeC_x films should not be damaged mechanically.

5. Conclusions

In most cases, MeC_x films protect the Al film underneath from reacting with applied Galinstan. However, the MeC_x films are sensitive to mechanical damages, which is also observed for Al films. By scratching with a pipette tip or sweeping Galinstan drops by glove-protected hand would result in corrosion reactions to take place. It was shown with XPS analysis that no chemical changes have occurred upon scratching the MeC_x surface and its' oxide layer, which lead to the conclusion of mechanical damages causing reactions to take place. It is suggested that this mechanical damage causes the MeC_x film to fissure, which enables Galinstan to diffuse through the MeC_x film and react with the underlying Al film.

It was seen that the reaction between Galinstan and Al would be enhanced with water (humidity). This is believed because water is able to reduce Ga easier than oxygen would. If the condensation of water was prevented, reaction between Galinstan and Al would not occur as easily.

There are differences between each examined MeC_x film. It was seen that the $\text{Cr-C}_{\text{poor}}$ film resisted Galinstan better than the other MeC_x films. This film has a low adhesion towards Galinstan and has resisted corrosion with Al to take place despite mild mechanical damages, unlike the other MeC_x films. Possible reasons for this can be a smooth surface morphology, relatively low hardness of the Cr-C films and therefore higher flexibility, as well as the lack of crystalline grains. Zr-C and $\text{Cr-C}_{\text{rich}}$ films also provide with resistance towards Galinstan, while Ti-C and Nb-C do not.

This study cannot propose any evident applications of Galinstan and the tested MeC_x films, which needs to be studied further. Such studies could involve testing the reactivity of Galinstan under electric current or electromagnetic fields. Some experiments could be improved by using a camera for recording rather than photographing.

6. Acknowledgements

The author would like to thank Erik Lewin for his supervision throughout the project, including the deposition of the MeC_x films, helping out with the XPS analysis and carefully reading through this work several times. The author would also like to thank Patrik Ahlberg for providing with the Galinstan used in this project as well as useful articles about the topic and tips for framing the lab set-up. Many thanks to Martin Häggblad Sahlberg for reading this work and questioning it to a critical extent. Thanks also goes to the fellow degree project worker students (K5, Q5) who have been a pleasant company throughout the time spent on this project. Lastly, thanks to the people who have contributed in assistance for XRD analysis as well as providing with the camera and furnace.

7. References

- [1] S. Cheng, Z. Wu, *Microfluidic electronics*, *Lab Chip*, 2012, 12, 2782-2791
- [2] H. Hollerith, *The Electric Tabulating Machine*, *Journal of the Royal Statistical Association*, Vol.57 Part 4, 1894
- [3] http://www.rgmd.com/thermometer_faq.html 2014-05-20 19:40
- [4] H. Hu et al., *Super flexible sensor skin using liquid metal as interconnect*, *IEEE SENSORS*, 2007 Conference
- [5] Geratherm Medical AG, *Safety Data Sheet acc. to Guideline 93/112/EC*, 2004
- [6] L. Guangyong et al., *PDMS based coplanar microfluidic channels for the surface reduction of oxidized Galinstan*, *Lab Chip*, 2014, 14, 200
- [7] T. Liu et al., *Characterization of Nontoxic Liquid-Metal Alloy Galinstan for Applications in Microdevices*, *Journal of Microelectromechanical Systems*, Vol 21, 2012
- [8] D.S. Evans, A. Prince, *Thermal analysis of Ga-In-Sn system*, *Metal Science*, 1978
- [9] M. Hodes et al., *On the Potential of Galinstan-Based Minichannel and Minigap Cooling*, *IEEE Transactions on Components, Packaging and Manufacturing Technology*, Vol 4, 2014
- [10] F. Scharmann et al., *Viscosity effect on GaInSn studied by XPS*, *Surface and Interface Analysis*, Vol 36, 2004
- [11] K.H.J Buschow, R.W. Cahn, M.C. Flemings, B. Ilschner, E.J. Kramer, S. Mahajan, *Encyclopedia of Materials – Science and Technology*, Volumes 1-11, Elsevier, 2001, Aluminum alloys: Properties and Applications
- [12] C. Nordling, J. Österman, *Physics handbook*, 8th ed. Studentlitteratur, 2006, table T2-1
- [13] R. Bruce King, *Encyclopedia of Inorganic Chemistry*, John Wiley & Sons Ltd. 1994, p519
- [14] H. Moissan, *Préparation au four électrique de quelques métaux réfractaires: tungstène, molybdène, Vanadium*, C R., 1893
- [15] G. Aylward, T. Findlay, *SI Chemical Data*, 6th ed., John Wiley & Sons Ltd. 2008, table 5
- [16] U. Jansson, E. Lewin, *Sputter deposition of transition-metal carbide films – A critical review from a chemical perspective*, *Thin Solid Films*, 2013
- [17] A.A. Öchsner, W. Ali, N., *Nanocomposite Coatings and Nanocomposite Materials*, Trans Tech Publications Ltd., 2009, chapter 1
- [18] M. Andersson et al., *Deposition and characterization of magnetron sputtered amorphous Cr-C films*, *Vacuum*, Vol 86, 2012
- [19] F. Franks, *Freeze-drying of Pharmaceuticals and Biopharmaceuticals*, Royal Society of Chemistry, 2007, chapter 6
- [20] W.D Callister, D.G. Rethwisch, *Materials Science and Engineering*, 8th ed., John Wiley & Sons Ltd., 2011, chapter 4
- [21] Swanson, Tatge. *Natl. Bur. Stand. (U.S.)*, Circ. 539 I, 11 (1953). Crystal Structure Source: LPF.
- [22] A.R. West, *Basic Solid State Chemistry*, 2nd ed., John Wiley & Sons Ltd., 2012, chapter 3
- [23] *Natl. Bur. Stand. (U.S.) Monogr.* 25 21, 60 (1985). Crystal Structure Source: LPF.
- [24] *Natl. Bur. Stand. (U.S.) Monogr.* 25 21, 62 (1985). Crystal Structure Source: LPF.
- [25] Bosio, L., Defrain, A., *Acta Crystallogr., Sec. B*, volume 25, page 995 (1969). Calculated from ICSD using POWD-12++ (1997)
- [26] Swanson, H.E., Fuyat, *Natl. Bur. Stand. (U.S.)*, Circ. 539, volume 539, page 3 (1954)
- [27] Lee, J.A., Raynor, G.V., *Nature (London)*, volume 174, page 1011 (1954). Calculated from ICSD using POWD-12++ (1997)
- [28] *Natl. Bur. Stand. (U.S.) Monogr.* 25 18, 73 (1981). Crystal Structure Source: LPF. Crystal Structure Source: LPF
- [29] Wong-Ng, W., McMurdie, H., Paretzkin, B., Hubbard, C., Dragoo, A., NBS, Gaithersburg, MD, USA. ICDD Grant-in-Aid (1986). Crystal Structure Source: LPF
- [30] *Natl. Bur. Stand. (U.S.) Monogr.* 25 21, 135 (1985). Crystal Structure Source: LPF
- [31] G. Aylward, T. Findlay, *SI Chemical Data*, 6th ed., John Wiley & Sons Ltd. 2008, table 11
- [32] W.D Callister, D.G. Rethwisch, *Materials Science and Engineering*, 8th ed., John Wiley & Sons Ltd., 2011, chapter 12